Adji Mama Marigo[1,2], Eulàlia Delgado[3], Jordi Torres[1,2], Cheikh Tidiane Bâ[4], Jordi Miquel[1,2,*]

Spermiogenesis and spermatozoon ultrastructure of the bothriocephalidean cestode Clestobothrium crassiceps (Rudolphi, 1819), a parasite of the teleost fish Merluccius merluccius (Gadiformes: Merlucciidae)

[1]Laboratori de Parasitologia, Departament de Microbiologia i Parasitologia Sanitàries, Facultat de Farmàcia, Universitat de Barcelona, Av. Joan XXIII, sn, E08028 Barcelona, Spain; [2]Institut de Recerca de la Biodiversitat, Facultat de Biologia, Universitat de Barcelona, Av. Diagonal, 645, E08028 Barcelona, Spain; [3]Departament de Ciències Ambientals, Facultat de Ciències, Universitat de Girona, Campus de Montilivi, sn, E17071 Girona, Spain; [4]Laboratoire de Parasitologie, Département de Biologie animale, Faculté des Sciences, Université Cheikh Anta Diop de Dakar, Dakar, Senegal

[*]Corresponding author: Jordi Miquel

Email: jordimiquel@ub.edu

Phone: + 34 93 402 45 00

Fax: + 34 93 402 45 04

Abstract

Spermiogenesis and the ultrastructure of the spermatozoon of the bothriocephalidean cestode Clestobothrium crassiceps (Rudolphi, 1819), a parasite of the teleost fish Merluccius merluccius (Linnaeus, 1758), have been studied by means of transmission electron microscopy. Spermiogenesis involves firstly the formation of a differentiation zone. It is characterized by the presence of two centrioles associated with striated rootlets, an intercentriolar body and an electron-dense material in the apical region of this zone. Later, two flagella develop from the centrioles, growing orthogonally in relation to the median cytoplasmic process. Flagella then undergo a rotation of 90° until they become parallel to the median cytoplasmic process, followed by the proximodistal fusion of the flagella with the median cytoplasmic process. The nucleus elongates and afterwards it migrates along the spermatid body. Spermiogenesis finishes with the appearance of the apical cone surrounded by the single helical crested body at the base of the spermatid. Finally, the narrowing of the ring of arched membranes detaches the fully formed spermatozoon. The mature spermatozoon of C. crassiceps is filiform and contains two axonemes of the 9+"1" trepaxonematan pattern, a parallel nucleus, parallel cortical microtubules and electron-dense granules of glycogen. The anterior extremity of the gamete exhibits a short electron-dense apical cone and one crested body, which turns once around the sperm cell. The first axoneme is surrounded by a ring of thick cortical microtubules that persist until the appearance of the second axoneme. Later, these thick cortical microtubules disappear and thus, the mature spermatozoon exhibits two bundles of thin cortical microtubules. The posterior extremity of the male gamete presents only the nucleus. Results are discussed and compared particularly with the available ultrastructural data on the former "pseudophyllideans". Two differences can be stablished between spermatozoa of Bothriocephalidea and Diphyllobothriidea, the type of spermatozoon (II vs I) and the presence/absence of the ring of cortical microtubules.

Keywords: Spermiogenesis, Spermatozoon, ultrastructure, Clestobothrium crassiceps, Bothriocephalidea, Cestoda

Introduction

The genus Clestobothrium is included in the recent tapeworm order Bothriocephalidea, which had formerly been included in the suppressed order "Pseudophyllidea" (Kuchta et al. 2008a). In their study Kuchta et al. (2008a) showed that the order Pseudophyllidea consists of two unrelated clades using molecular, morphological, and ecological approaches. The ultrastructural spermatological data available to date support these results and confirm the existence of important ultrastructural differences between the species of both orders (Levron et al. 2005, 2006a,b,c, 2009; Bâ et al. 2007; Bruňanská et al. 2010; Šípková et al. 2010, 2011). Bothriocephalideans are intestinal parasites of teleost fishes including 46 genera distributed into four families (Bothriocephalidae, Echinophallidae, Philobythiidae and Triaenophoridae). The genus Clestobothrium is included in the Bothriocephalidae along with another 13 valid genera (Kuchta et al. 2008a,b). Morphologically, individuals belonging to the genus Clestobothrium differ from other bothriocephalids because they possess a sphincter surrounding the anterior aperture of bothria (Schmidt 1986; Bray et al. 1994). To date, this genus comprises only three valid species: (1) Clestobothrium crassiceps, the genus type species that was initially described as Bothriocephalus crassiceps, (2) Clestobothrium gibsoni, formerly described as Bathygadus macrops, and (3) Clestobothrium neglectum, described as Raniceps raninus (Kuchta et al. 2008b). The remaining families of Bothriocephalidea include eight genera in the Echinophallidae, two genera in the Philobythiidae and 22 genera in the Triaenophoridae (Kuchta et al. 2008a,b).

The usefulness of ultrastructural data of spermiogenesis and the spermatozoon to elucidate the phylogenetic relationships within the Platyhelminthes has been demonstrated by several authors (Euzet et al. 1981; Justine 1991, 1998, 2001; Bâ and Marchand 1995; Levron et al. 2010). To our knowledge, the spermatological characters of only 13 species of the former "Pseudophyllidea" have been studied, including 10 bothriocephalideans and three diphyllobothriideans. Concerning the bothriocephalideans the analysed species are the bothriocephalids Bothriocephalus clavibothrium, Bothriocephalus claviceps, Bothriocephalus scorpii, Oncodiscus sauridae and Senga sp. (Świderski and Mokhtar-Maamouri 1980; Levron et al. 2006b; Bâ et al. 2007; Šípková et al. 2011), the echinophallids Parabothriocephalus gracilis and Paraechinophallus japonicus (Levron et al. 2006a; Šípková et al. 2010), and the triaenophorids Eubothrium crassum, Eubothrium rugosum and Triaenophorus nodulosus (Bruňanská et al. 2001, 2002, 2010; Levron et al. 2005). In what refers the diphyllobothriideans, the three studied species are the scyphocephalid Duthiersia fimbriata (Justine 1986), and the diphyllobothriids Diphyllobothrium latum and Ligula intestinalis (Levron et al. 2006c, 2009).

The present study describes for the first time the spermiogenesis and the spermatozoon ultrastructure of Clestobothrium crassiceps, with the aim of providing new data on this genus potentially useful for phylogenetic analyses.

Materials and methods

Live adult specimens of Clestobothrium crassiceps were collected from the intestine of the teleost fish Merluccius merluccius (Gadiformes: Merlucciidae) caught in Roses (Girona, Spain).

Live cestodes were first placed in a 0.9% NaCl solution. Later the mature proglottids were fixed in cold (4°C) 2.5% glutaraldehyde in a 0.1 M sodium cacodylate buffer at pH 7.4 for a minimum of 2h, rinsed in a 0.1 M sodium cacodylate buffer at pH 7.4, postfixed in cold (4°C) 1% osmium tetroxide in the same buffer for 1 h, rinsed in a 0.1 M sodium cacodylate buffer at pH 7.4, dehydrated in an ethanol series and propylene oxide, and finally embedded in Spurr's resin. Ultrathin sections were obtained using a Reichert-Jung Ultracut E ultramicrotome, placed on copper grids and double-stained with uranyl acetate and lead citrate (Reynolds 1963). Ultrathin sections were examined using a JEOL 1010 TEM operated at an accelerating voltage of 80 kV.

The presence of glycogen was detected using the method of Thiéry (1967). Gold grids were treated in periodic acid, thiocarbohydrazide, and silver proteinate (PA-TCH-SP) as follows: 30 min in 10% PA, rinsed in distilled water, 24h in TCH, rinsed in acetic solutions and distilled water, 30 min in 1 % SP in the dark, and rinsed in distilled water.

Results

Spermiogenesis (Figs. 1 to 4)

In the testes, spermatids are grouped in rosettes and are interconnected to a central cytophore by cytoplasmic bridges (Fig. 1a). Each spermatid contains a large nucleus with scattered chromatin and numerous mitochondria (Fig. 1a). Spermiogenesis starts by the formation of a zone of differentiation situated at the periphery of each spermatid (Fig. 1b). In the very early stages of spermiogenesis it is possible to observe an electron-dense material in the peripheral region of the zone of differentiation (Fig. 1b). The differentiation zone also contains two centrioles associated with striated rootlets and an intercentriolar body (Fig. 1b-d). The intercentriolar body is a cylindrical structure and consists of three electron-dense plates: one

central thicker electron-dense layer bordered by two thin electron-dense layers (Fig. 1c). The differentiation zone is lined by a layer of submembranous cortical microtubules and delimited at its base by a ring of arched membranes (Fig. 1d). Cross-sections of this zone show that cortical microtubules are associated with an electron-dense material organized in several submembranous fields (Fig. 1c). In longitudinal sections, this electron-dense material is also visible and extends up to the ring of arched membranes (Fig. 1d). One of the centrioles elongates and gives rise to a flagellum (Fig. 1e). Later the second flagellum also elongates and, thus, two flagella of unequal length are formed perpendicularly to an incipient median cytoplasmic process (Fig. 1f). It is interesting to note that the growth of the flagella is asynchronous (Figs. 1e,f; 2a). Later, both flagella undergo a rotation of 90° and become parallel to the median cytoplasmic process (Fig. 2b-d). At this stage, four very small accumulations of electron-dense material, the so-called attachment zones, appear on the inner surface of the plasma membrane in the median cytoplasmic process (Fig. 2c). These attachment points mark the lines where the fusion of the median cytoplasmic process with the two axonemes takes place.

Thus, both axonemes fuse with the cytoplasmic extension in a proximodistal way (Fig. 2e). The nucleus, located outside the ring of arched membranes, forms a cone-like extension directed towards the elongated spermatid (Fig. 2f). It is important to note that, after the proximodistal fusion, the axonemes become longitudinally displaced in relation to one another and striated rootlets are still present (Fig. 2f). Afterwards, the nucleus elongates and migrates into the spermatid (Fig. 3a). At the final stages of spermiogenesis, the ring of arched membranes narrows (Fig. 3b,c). The crested body and the future apical cone become visible only at the very end of spermiogenesis (Fig. 3c), just before the detachment of the mature spermatozoon from the residual cytoplasm.

Spermatozoon (Figs. 5 to 7)

The mature spermatozoon of Clestobothrium crassiceps is filiform, tapered at both ends, and lacks mitochondria. From the anterior to the posterior extremities, four regions can be distinguished on the basis of distinctive ultrastructural features.

Region I (Figs. 5a-h, 7I) constitutes the anterior extremity of the spermatozoon. It exhibits a small apical cone of electron-dense material, measuring 620 nm, surrounded by the single helical crested body (Fig. 5a,b). The crested body, 160 nm thick, is also short and describes only one turn around the sperm cell (Fig. 5a). At the anterior tip of the cell some microtubules become gradually visible from the apical cone area to the centriole area (Fig. 5b-e). Thus, these microtubules progressively form an arc of cortical microtubules beneath the plasma membrane and finally, when the first axoneme appears, they constitute a complete ring of about 24 to 30 parallel submembranous cortical microtubules that encircles the axoneme (Fig. 5f-h). These cortical microtubules are characterized by a thick membrane and an electron-lucent centre and they extend up to Region II of the spermatozoon containing the second centriole (Fig. 5f-k). The axoneme shows the 9+"1" pattern of the trepaxonematan Platyhelminthes (Fig. 5f-h).

Region II (Figs. 5i-n, 6a, 7II) lacks crested body and is characterized by the presence of two axonemes of the 9+"1" trepaxonematan pattern and also by the appearance of electron-dense granules of glycogen (Figs. 5l-n, 6a). At the end of Region I, scattered electron-dense microtubular elements appear indicating the beginning of the second centriole (Fig. 5i-k). At the same time, the ring of thick electron-dense cortical microtubules disorganizes and finally disappears (Fig. 5j,k). At this level, both axonemes are very close to each other being separated by two thin electron-dense cortical microtubules (Fig. 5l). At this level, four

electron-dense points corresponding to the attachment zones are visible in cross-sections (Fig. 5l). Subsequently, the width of the spermatozoon increases, the cortical microtubules become arranged in two opposite parallel fields of four units, and electron-dense granules appear between them (Fig. 5m,n). The method of Thiéry reveals that these electron-dense granules are glycogen (Fig. 6a).

Region III (Figs. 6b-d, 7III) contains two axonemes, electron-dense granules of glycogen, and two fields of submembranous and parallel cortical microtubules. This region is characterized by the beginning of the nucleus by the presence of the anterior part of nucleus (Fig. 6b). The nucleus is electron-dense with fibrillar patches of chromatin (Fig. 6c). Afterwards, the diameter of the nucleus increases gradually (Fig. 6b-d). Each field of parallel cortical microtubules is composed by seven to eight units. At the end of this region, one of the axonemes starts to disorganize and finally disappears (Fig. 6c,d).

Region IV (Figs. 6e-j, 7IV) is characterized by the presence of one axoneme, nucleus (posterior part), electron-dense granules of glycogen, and parallel cortical microtubules. Cortical microtubules are still organized in two fields, composed of five to six units (Fig. 6e). They gradually disappear in the posterior part of this region, near the posterior extremity of the spermatozoon (Fig. 6e,f). The diameter of the nucleus increases at this level and reaches its maximum size (Fig. 6e). At the posterior part of the spermatozoon, the nucleus decreases in diameter and cortical microtubules disappear (Fig. 6f). Later the axoneme disorganizes: the central core disappears and doublets lose their arms (Fig. 6g), become disorganized, and finally they transform into singlets (Fig. 6h). At this level the nucleus subsists along with only a few singlets (Fig. 6h). The posterior extremity of the gamete is characterized by the nucleus surrounded by the plasma membrane (Fig. 6i,j).

Discussion

Spermiogenesis

There are some particularities in the spermiogenesis of the former "Pseudophyllidea" when comparing with the spermiogenesis of other orders of cestodes. For example, one of such particularities is the accumulation of electron-dense material in the apical area of the differentiation zone during the early stages of spermiogenesis. This electron-dense material, described for the first time in Eubothrium crassum (Bruňanská et al. 2001), has also been reported in caryophyllideans (Bruňanská and Poddubnaya 2006; Miquel et al. 2008; Bruňanská 2009; Yoneva et al. 2011) and spathebothriideans (Bruňanská et al. 2006; Bruňanská and Poddubnaya 2010), being present only during the initial stages of spermiogenesis. This electron-dense material has also been observed in Clestobothrium crassiceps in our study. According to Bruňanská and Poddubnaya (2010), this feature can be regarded as characteristic of the basal or lower eucestodes. It is also important to note that in all the studied species of the former "Pseudophyllidea" the cortical microtubules are associated with another electron-dense material present during spermiogenesis. Although this electron-dense material is observed in all the studied Bothriocephalidea and Diphyllobothriidea, it is not mentioned by the authors in their studies (Świderski and Mokhtar-Maamouri 1980; Justine 1986; Bruňanská et al. 2001, 2002, 2010; Levron et al. 2005, 2006a,b,c, 2009; Bâ et al. 2007; Šípková et al. 2010, 2011). However, the localization of the electron-dense material in the differentiation zone of cestodes during spermiogenesis is sometimes restricted to the centriolar areas, as it happens for example in certain cyclophyllideans presenting the so-called centriolar adjunct or centriole associated structures (Bâ et al. 1991, 2000; Bâ and Marchand 1994, 1998; Miquel et al. 2005; Eira et al. 2006). Moreover, in some of these cyclophyllideans, such as Gallegoides arfaai or Mosgovoyia

Eliminado: orders

ctenoides, the electron-dense structures associated with centrioles are still present when the axonemes are already formed (Miquel et al. 2005; Eira et al. 2006).

The process of spermiogenesis in C. crassiceps is characterized by a flagellar rotation and proximodistal fusion. This type of spermiogenesis corresponds to the "Pseudophyllidean type" of Świderski (1986) or to the type I of Bâ and Marchand (1995). It is important to remark that members of the two unrelated clades that constituted the former order Pseudophyllidea (Bothriocephalidea and Diphyllobothriidea) follow the type I of spermiogenesis (see Table I). Thus, taking into account that the four types of spermiogenesis stablished by Bâ and Marchand (1995) are the major characteristics of spermiogenesis in the eucestodes and that members of the two orders show the same pattern, future studies of spermiogenesis should be focussed on characters such as intercentriolar body, particularly for the diphyllobothriideans due to the scarce available data in this order.

The intercentriolar body is a character used in phylogenetic studies for the classification of higher-level cestodes (Hoberg et al. 1997; Justine 2001; Olson et al. 2001; Levron et al. 2010). The intercentriolar body in C. crassiceps includes three electron-dense layers delimited by four electron-lucent layers. This character is variable within the "Pseudophyllidea" and the number of plates varies from one to five within the group. It is formed by a single electron-dense layer in both B. scorpii and E. crassum (Bruňanská et al. 2001; Levron et al. 2006b), by three layers in P. gracilis, T. nodulosus and D. latum (Levron et al. 2005, 2006c; Šípková et al. 2010) as occurs in C. crassiceps, and by five layers in L. intestinalis (Levron et al. 2009). According to Justine (2001), a progressive reduction of the intercentriolar body occurs in the higher cestodes.

Spermatozoon

Recent studies on cestode spermatozoa have revealed numerous new ultrastructural characters showing a great degree of variation. These numerous supplementary characters are constantly increasing the degree of utility of spermatozoon ultrastructure for analysis of cestode phylogeny and evolution (Hoberg et al. 1997, 1999; Justine 2001; Olson et al. 2001; Levron et al. 2010).

The spermatozoon of C. crassiceps also shows particular characters. It possesses two axonemes of the 9+"1" trepaxonematan pattern, a single crested body, parallel nucleus and parallel cortical microtubules. Therefore it corresponds to the type II spermatozoon of Levron et al. (2010). This type has been reported in all the studied species of Bothriocephalidea (Świderski and Mokhtar-Maamouri 1980; Bruňanská et al. 2001, 2002, 2010; Levron et al. 2005, 2006a,b; Bâ et al. 2007; Šípková et al. 2010, 2011), Tetraphyllidea-Onchobothriidae (Mokhtar-Maamouri and Świderski 1975; Mokhtar-Maamouri 1982; Quilichini et al. 2007; Marigo et al. 2011a), Proteocephalidea (Sène et al. 1997; Bruňanská et al. 2003a,b; 2004a,b) and in two Diphyllidea (Azzouz-Draoui 1985).

An interesting feature in the spermatozoon of C. crassiceps is the presence of an apical cone in its anterior extremity. Among the 13 previously studied "pseudophyllideans" this structure was only described by Bâ et al. (2007) in Bothriocephalus claviceps. However, in B. claviceps, the apical cone is very long (around 6.6 μm) while in C. crassiceps this structure is short and measures about 600 nm.

The crested body is another structure that also marks the anterior part of the spermatozoon and is present in most but not all cestode spermatozoa. In the Bothriocephalidea, the crested

body is present in almost all studied species except for a single taxon, Bothriocephalus clavibothrium (Świderski and Mokhtar-Maamouri 1980). The presence of the crested body is considered a synapomorphy for the eucestodes (Bâ and Marchand 1995). Posteriorly, Justine (1998) proposed the crested body as a synapomorphy in derived groups of cestodes, including the Pseudophyllidea. Therefore, the crested body is presumably absent in the most basal eucestodes, i.e., Caryophyllidea, Spathebothriidea, Haplobothriidea and Trypanorhyncha (Levron et al. 2010). In light of the spermatozoon study presented here, as well as previous ones, the crested body is only present in bothriocephalidean cestodes, but not in diphyllobothriideans (see Table I).

Eliminado: Eucestoda
Eliminado: Ba
Eliminado: a synapomorphy
Eliminado: for
Eliminado: for

The anterior part of the spermatozoon of bothriocephalideans is characterized by the presence of a ring of thick electron-dense cortical microtubules encircling the axoneme (Świderski and Mokhtar-Maamouri 1980; Bruňanská et al. 2002, 2010; Levron et al. 2005, 2006a,b; Šípková et al. 2010, 2011). This feature has not been observed in the diphyllobothriideans Ligula intestinalis or D. latum (Levron et al. 2006c, 2009). However, an incomplete ring of cortical microtubules has been described in the diphyllobothriidean Duthiersia fimbriata (Justine 1986), but this observation requires confirmation. Later, in more posterior areas of the spermatozoon these cortical microtubules become thin and, consequently two types of microtubules have been observed: the first type (thick cortical microtubules) forms the ring and is localised in the anterior part, and the second type (thin cortical microtubules) is localised posteriorly (Świderski and Mokhtar-Maamouri 1980; Bruňanská et al. 2002, 2010; Levron et al. 2005, 2006a,b; Šípková et al. 2010, 2011). Among the Bothriocephalidae some species present particularities such as those in B. claviceps (Bâ et al. 2007) presenting a partial ring of cortical microtubules. Also, in E. crassum cortical microtubules had been initially attributed to a posterior area of the sperm cell (Bruňanská et al. 2002). Nonetheless,

Eliminado: appears
Eliminado: when the first type disappears

sections containing the ring of cortical microtubules were recently attributed to the anterior region of the spermatozoon (Bruňanská et al. 2010). In Triaenophorus nodulosus, Bothriocephalus scorpii and Eubothrium rugosum this ring of cortical microtubules participates in the formation of the crested body (Levron et al. 2005, 2006b; Bruňanská et al. 2010). On the other hand, the first type of cortical microtubules generally stays in the first region of the spermatozoon, but in B. claviceps (Bâ et al. 2007) some electron-dense microtubules were found in the posterior areas of the sperm cell. According to Šípková et al. (2010) this ring of electron-dense cortical microtubules is only described in the spermatozoa of bothriocephalideans and may indicate a suitable spermatozoon character for recognition of divergent taxa. On the other hand, Levron et al. (2010) considered the ring of electron-dense cortical microtubules as a possible autapomorphy for the Bothriocephalidea. This fact is confirmed in the study of Oncodiscus sauridae and Senga sp, (Šípková et al. 2011) and also in C. crassiceps in the present study.

Con formato: Subrayado
Con formato: Subrayado
Con formato: Subrayado

The attachment zones indicate the area of fusion of the two free flagella with the median cytoplasmic process during spermiogenesis. These structures, observed in C. crassiceps during the present study, are also described in six other Bothriocephalidea namely Paraechinophallus japonicus, Bothriocephalus scorpii, E. crassum, E. rugosum, Oncodiscus sauridae and Senga sp (Levron et al. 2006a,b; Bruňanská et al. 2010; Šípková et al. 2011), in two Diphyllobothriidea namely Ligula intestinalis and Diphyllobothrium latum (Levron et al. 2006c, 2009) and in three Trypanorhyncha namely Aporhynchus menezesi, Dollfusiella spinulifera and Parachristianella trygonis (Miquel and Świderski 2006, Miquel et al. 2007, Marigo et al. 2011b).

The posterior part of the spermatozoon of C. crassiceps as in D. latum (Levron et al. 2006c) shows only the nucleus. This posterior end in bothriocephalidean and diphyllobothriidean cestodes is variable even within the species and contains a nucleus, or a nucleus plus microtubules, or an axoneme (see Table I). According to this variability, the posterior extremity of the spermatozoon does not appear to possess characters suitable for differentiating members of Bothriocephalidea and Diphyllobothriidea.

Acknowledgements

We are grateful to the "Unitat de Microscòpia, Facultat de Medicina, Centres Científics i Tecnològics de la Universitat de Barcelona (CCiTUB)" for their support in the preparation of samples, particularly Núria Cortadellas and Almudena García. The present study was partially funded by the Spanish project CTM2009-08602. Adji Mama Marigo benefits from doctoral grants (2009-10 no 0000448124 and 2010-11 no 0000538056) of "Ministerio de Asuntos Exteriores y de Cooperación, Agencia Española de Cooperación Internacional para el Desarrollo MAEC-AECID".

References

Azzouz-Draoui N (1985) Étude ultrastructurale comparée de la spermiogenèse et du spermatozoïde de quatre Cestodes Diphyllidea. Thèse de 3º Cycle, Université de Tunis, Tunis, Tunisie.

Bâ A, Bâ CT, Marchand B (2000) Ultrastructure of spermiogenesis and the spermatozoon of Sudarikovina taterae (Cestoda, Cyclophyllidea, Anoplocephalidae) intestinal parasite of Tatera gambiana (Rodentia, Gerbillidae). J Submicrosc Cytol Pathol 32:137-144.

Bâ CT, Bâ A, Marchand B (2007) Ultrastructure of the spermatozoon of Bothriocephalus claviceps (Cestoda, Pseudophyllidea): a parasite of Anguilla anguilla (Fish, Teleostei). Parasitol Res 101:77-83. doi: 10.1007/s00436-006-0445-z

Bâ CT, Marchand B (1994) Ultrastructure of spermiogenesis and the spermatozoon of Mathevotaenia herpestis (Cestoda), intestinal parasite of Atelerix albiventrix in Sénégal. Acta Zool (Stock) 75:167-175. doi: 10.1111/j.1463-6395.1994.tb01120.x

Bâ CT, Marchand B (1995) Spermiogenesis, spermatozoa and phyletic affinities in the Cestoda. Mém Mus Natn Hist Nat 166:87-95.

Bâ CT, Marchand B (1998) Ultrastructure of spermiogenesis and the spermatozoon of Vampirolepis microstoma (Cestoda, Hymenolepididae), intestinal parasite of Rattus rattus. Microsc Res Techn 42:218-225.

Bâ CT, Marchand B, Mattei X (1991) Demonstration of the orientation of the Cestodes spermatozoon illustrated by the ultrastructural study of spermiogenesis of a Cyclophyllidea: Thysaniezia ovilla, Rivolta, 1874. J Submicrosc Cytol Pathol 23:605-612.

Bray RA, Jones A, Anderson KI (1994) Order Pseudophyllidea Carus, 1863. In: Khalil LF, Jones A, Bray RA, editors. Key to the cestode parasites of vertebrates, Wallingford: CAB International, p. 205-247.

Bruňanská M (2009) Spermatological characters of the caryophyllidean cestodes Khawia sinensis Hsü, 1935, a carp parasite. Parasitol Res 105:1603-1610. doi: 10.1007/s00436-009-1599-2

Bruňanská M, Fagerholm HP, Nebesářová J, Kostič B (2010) Ultrastructure of the mature spermatozoon of Eubothrium rugosum (Batsch, 1786) with a re-assessment of the spermatozoon ultrastructure of Eubothrium crassum (Bloch, 1779) (Cestoda: Bothriocephalidea). Helminthologia 47:257-263. doi: 10.2478/s11687-010-0040-9

Bruňanská M., Nebesářová J., Scholz T. (2003a). Ultrastructure of the spermatozoon of the proteocephalidean cestode Proteocephalus torulosus (Batsch, 1786). Parasitol Res 89:345-351. doi: 10.1007/s00436-002-0757-6

Bruňanská M, Nebesářová J, Scholz T Fagerholm HP (2001) Spermiogenesis in the pseudophyllid cestode Eubothrium crassum (Bloch, 1779). Parasitol Res 87:579-588. doi: 10.1007/s004360100392

Bruňanská M, Nebesářová J, Scholz T, Fagerholm HP (2002) Ultrastructure of the spermatozoon of the pseudophyllidean cestode Eubothrium crassum (Bloch, 1779). Parasitol Res 88:285-291. doi: 10.1007/s00436-001-0532-0

Bruňanská M, Poddubnaya LG (2006) Spermiogenesis in the caryophyllidean cestode Khawia armeniaca (Cholodkovski, 1915). Parasitol Res 99:449-454. doi: 10.1007/s00436-006-0155-6

Bruňanská M, Poddubnaya LG (2010) Spermatological characters of the spathebothriidean tapeworm Didymobothrium rudolphii (Monticelli, 1890) Parasitol Res 106:1435-1442. doi: 10.1007/s00436-010-1822-1

Bruňanská M, Scholz T, Dezfuli BS, Poddubnaya LG (2006) Spermiogenesis and sperm ultrastructure of Cyathocephalus truncatus (Pallas 1781) Kessler 1868 (Cestoda: Spathebothriidea). J Parasitol 92:884-892. doi: 10.1645/GE-718R1.1

Bruňanská M, Scholz T, Ibraheem MH (2004a) Ultrastructural characters of the spermatozoon of the cestode Corallobothrium solidum Fritsch, 1886 (Cestoda: Proteocephalidea), a parasite of the electric catfish Malapterurus electricus. Parasitol Res 94:421-426. doi: 10.1007/s00436-004-1236-z

Bruňanská M, Scholz T, Ibraheem MH (2004b) Ultrastructural particularities of the spermatozoon of the cestode Electrotaenia malopteruri (Fritsch, 1886) (Proteocephalidae: Gangesiinae), a parasites of Malapterurus electricus

(Siluriformes: Malapteruridae) from the river Nile, Egypt. Parasitol Res 93:114-120. doi: 10.1007/s00436-004-1109-5

Bruňanská M, Scholz T, Nebesářová J (2003b) Reinvestigation of the spermatozoon ultrastructure of the cestode Proteocephalus longicollis (Zeder, 1800), a parasite of salmonid fish. Parasitol Res 91:357-362. doi: 10.1007/s00436-003-0977-4

Eira C, Miquel J, Vingada J, Torres J (2006) Spermiogenesis and spermatozoon ultrastructure of the cestode Mosgovoyia ctenoides (Cyclophyllidea: Anoplocephalidae), an intestinal parasite of Oryctolagus cuniculus (Lagomorpha: Leporidae). J Parasitol 92:708-718. doi: 10.1645/GE-818R.1

Euzet L, Świderski Z, Mokhtar-Maamouri F (1981) Ultrastructure comparée du spermatozoïde des Cestodes. Relations avec la phylogénèse. Ann Parasitol (Paris) 56:247-259.

Hoberg EP, Gardner SL, Campbell RA (1999) Systematics of the Eucestoda: advances toward a new phylogenetic paradigm, and observations on the early diversification of tapeworms and vertebrates. Syst Parasitol 42:1-12. doi: 10.1023/A:1006099009495

Hoberg EP, Mariaux J, Justine J-L, Brooks DR, Weekes PJ (1997) Phylogeny of the orders of the Eucestoda (Cercomeromorphae) based on comparative morphology: historical perspectives and a new working hypothesis. J Parasitol 83:1128-1147.

Justine J-L (1986) Ultrastructure of the spermatozoon of the cestode Duthiersia fimbriata (Pseudophyllidea, Diphyllobothriidae). Can J Zool 64:1545-1548.

Justine J-L (1991) Phylogeny of parasitic Platyhelminthes: a critical study of synapomorphies proposed on the basis of the ultrastructure of spermiogenesis and spermatozoa. Can J Zool 69:1421-1440.

Justine J-L (1998) Spermatozoa as phylogenetic characters for the Eucestoda. J Parasitol 84:385-408. doi: 10.2307/3284502

Justine J-L (2001) Spermatozoa as phylogenetic characters for the Platyhelminthes. In: Littlewood DTJ and Bray RA (eds), Interrelationships of the Platyhelminthes. Taylor and Francis, London. pp 231-238.

Kuchta R, Scholz T, Brabec J, Bray RA (2008a) Suppression of the tapeworm order Pseudophyllidea (Platyhelminthes: Eucestoda) and the proposal of two new orders, Bothriocephalidea and Diphyllobothriidea. Int J Parasitol 38:49-55. doi:10.1016/j.ijpara.2007.08.005

Kuchta R, Scholz T, Bray RA (2008b). Revision of the order Bothriocephalidea Kuchta, Scholz, Brabec & Bray, 2008 (Eucestoda) with amended generic diagnoses and keys to families and genera. Syst Parasitol 71:81-136. doi: 10.1007/s11230-008-9153-7

Levron C, Bruňanská M, Kuchta R, Freeman M, Scholz T (2006a) Spermatozoon ultrastructure of the pseudophyllidean cestode Paraechinophallus japonicus, a parasite of deep-sea fish Psenopsis anomala (Perciformes, Centrolophidae). Parasitol Res 100:115-121. doi: 10.1007/s00436-006-0224-x

Levron C, Bruňanská M, Marchand B (2005) Spermiogenesis and sperm ultrastructure of the pseudophyllidean cestode Triaenophorus nodulosus (Pallas, 1781) Parasitol Res 98:26-33. doi: 10.1007/s00436-005-0009-7

Levron C, Bruňanská M, Poddubnaya LG (2006b) Spermatological characters of the pseudophyllidean cestode Bothriocephalus scorpii (Muller, 1781). Parasitol Int 55:113-120. doi: 10.1016/j.parint.2005.11.055

Levron C, Bruňanská M, Poddubnaya LG (2006c) Spermatological characters in Diphyllobothrium latum (Cestoda, Pseudophyllidea). J Morphol 267:1110-1119. doi: 10.1002/jmor.10460

Levron C, Miquel J, Oros M, Scholz T (2010) Spermatozoa of tapeworms (Platyhelminthes, Eucestoda): advances in ultrastructural and phylogenetic studies. Biol Rev 85:523-543. doi: 10.1111/j.1469-185X.2009.00114.x

Levron C, Sítko J, Scholz T (2009) Spermiogenesis and spermatozoon of the tapeworm Ligula intestinalis (Diphyllobothriidea): phylogenetic implications. J Parasitol 95:1-9. doi: 10.1645/GE-1646.1

Marigo AM, Eira C, Bâ CT, Miquel J (2011a) Spermatological characters of Acanthobothrium crassicolle Wedl, 1855 (Tetraphyllidea, Onchobothriidae), a parasite of the common stingray Dasyatis pastinaca. Acta Parasitol (in press). doi: 10.2478/s11686-011-0025-y

Marigo AM, Świderski Z, Bâ CT, Miquel J (2011b) Spermiogenesis and ultrastructure of the spermatozoon of the trypanorhynch cestode Aporhynchus menezesi (Aporhynchidae), a parasite of the velvet belly lanternshark Etmopterus spinax (Elasmobranchii: Etmopteridae). Folia Parasitol 58:69-78.

Miquel J, Świderski Z (2006) Ultrastructure of the spermatozoon of Dollfusiella spinulifera (Beveridge and Jones, 2000) Beveridge, Neifar and Euzet, 2004 (Trypanorhyncha, Eutetrarhynchidae). Parasitol Res 99:37-44. doi: 10.1007/s00436-005-0094-7

Miquel J, Świderski Z, Mackiewicz JS and Ibraheem MH (2008) Ultrastructure of spermiogenesis in the caryophyllidean cestode Wenyonia virilis Woodland, 1923, with re-assessment of flagellar rotation in Glaridacris catostomi Cooper, 1920. Acta Parasitol 53:19-29. doi: 10.2478/s11686-008-0013-z

Miquel J, Świderski Z, Młocicki D, Eira C, Marchand B (2005) Spermatogenesis in the anoplocephalid cestode Gallegoides arfaai (Mobedi et Ghadirian, 1977) Tenora et Mas-Coma, 1978. Acta Parasitol 50:132-144. doi: 10.1007/s00436-004-1238-x

Eliminado: (in press)

Miquel J, Świderski Z, Neifar L, Eira C (2007) Ultrastructure of the spermatozoon of Parachristianella trygonis Dollfus, 1946 (Trypanorhyncha, Eutetrarhynchidae). J Parasitol 93:1296-1302. doi: 10.1645/GE-1193.1

Mokhtar-Maamouri F (1982) Étude ultrastructurale de la spermiogenèse de Acanthobothrium filicolle var. filicolle Zschokke, 1888 (Cestoda, Tetraphyllidea, Onchobothriidae). Ann Parasitol (Paris) 57:429-442.

Mokhtar-Maamouri F, Świderski Z (1975) Étude en microscopie électronique de la spermatogénèse de deux Cestodes Acanthobothrium filicolle benedenii Loennberg, 1889 et Onchobothrium uncinatum (Rud., 1819) (Tetraphyllidea, Onchobothriidae). Z Parasitenkd 47:269-281. doi: 10.1007/BF00389886

Olson PD, Littlewood DTJ, Bray RA, Mariaux J (2001) Interrelationships and evolution of the tapeworm (Platyhelminthes: Cestoda). Mol Phylogenet Evol 19:443-467. doi: 10.1006/mpev.2001.0930

Quilichini Y, Foata J, Bâ CT, Marchand B (2007) Ultrastructure of the spermatozoon of Calliobothrium verticillatum (Cestoda, Tetraphyllidea, Oncobothriidae). Acta Parasitol 52:219-224. doi: 10.2478/s11686-007-0037-9

Reynolds ES (1963) The use of lead citrate at high pH as an electron-opaque stain in electron microscopy. J Cell Biol 17:208-212.

Schmidt GD (1986) CRC handbook of tapeworm identification. Boca Raton: CRC Press, 1986, p. 675.

Sène A, Bâ CT, Marchand B (1999) Ultrastructure of spermiogenesis of Phyllobothrium lactuca (Cestoda, Tetraphyllidea, Phyllobothriidae). Folia Parasitol (Praha) 46:191-198.

Šípková L, Levron C, Freeman M, Scholz T (2010) Spermiogenesis and spermatozoon of the tapeworm Parabothriocephalus gracilis (Bothiocephalidea): Ultrastructural and cytochemical studies. Acta Parasitol 55:58-65. doi: 10.2478/s11686-010-0003-9

Šípková L, Levron C, Oros M, Justine J-L (2011) Spermatological characters of bothriocephalideans (Cestoda) inferred from an ultrastructural study on Oncodiscus sauridae and Senga sp. Parasitol Res (in press). doi: 10.1007/s00436-010-2215-1

Świderski Z (1986) Three types of spermiogenesis in cestodes. Proc XIth Int Cong Electron Microsc, Kyoto, Japan: 2959-2960.

Świderski Z, Mokhtar-Maamouri F (1980) Étude de la spermatogénèse de Bothriocephalus clavibothrium Ariola, 1899 (Cestoda: Pseudophyllidea). Arch Inst Pasteur Tunis 57:323-347.

Thiéry JP (1967) Mise en évidence des polysaccharides sur coupes fines en microscopie électronique. J Microsc 6:987-1018.

Yoneva A, Levron C, Oros M, Orosová M, Scholz T (2011) Ultrastructure of spermiogenesis and mature spermatozoon of Breviscolex orientalis (Cestoda: Caryophyllidea). Parasitol Res 108:997-1005. doi: 10.1007/s00436-010-2144-z

Legends of figures

Fig.1 Spermiogenesis in Clestobothrium crassiceps. **a** Rosette showing numerous peripheric spermatids attached to the central cytophore (Cy). M mitochondria, N nucleus. Bar 5 µm. **b** Longitudinal section of an early stage of spermiogenesis showing the appearance of the electron-dense material (DM). IB intercentriolar body, N nucleus, SR striated rootlets. Bar 0.5 µm. **c** Cross-section of the differentiation zone showing the intercentriolar body and the cortical microtubules (CM) associated with the electron-dense material (DM). Arrowheads

indicate the three electron-dense layers forming the intercentriolar body. SR striated rootlets. Bar 0.3 µm. **d** Longitudinal section of an early stage of spermiogenesis showing the presence of two centrioles (C), striated rootlets (SR), the intercentriolar body (IB) and the electron-dense material (DM) in the zone of differentiation. AM arched membranes, N nucleus. Bar 0.5 µm. **e, f** Two longitudinal sections of the differentiation zone confirming the asynchronic growth of the flagella. C2 second centriole, DM electron-dense material, F1 first flagellum, IB intercentriolar body, N nucleus. Bar 0.5 µm.

Fig. 2 Spermiogenesis in Clestobothrium crassiceps. **a** Longitudinal section of the zone of differentiation showing the unequal length of flagella (F1 first flagellum, F2 second flagellum) during the flagellar rotation. DM electron-dense material, N nucleus. Bar 0.5 µm **b** Longitudinal section of the zone of differentiation showing the two flagella (F) well developed. IB intercentriolar body, MCP median cytoplasmic process. Bar 0.5 µm. **c, d** Cross and longitudinal sections of the differentiation zone after the flagellar rotation. Note the presence of four attachment zones in the median cytoplasmic process (arrowheads). AM arched membranes, CM cortical microtubules, DM electron-dense material, F flagellum, MCP median cytoplasmic process Bar 0.3 µm, Bar 0.5 µm. **e** Longitudinal section of spermatid after the proximodistal fusion of axonemes (Ax). AM arched membranes. Bar 0.5 µm. **f** Longitudinal section at the beginning of the nuclear migration towards the cytoplasmic process. Note that the axonemes (Ax) are longitudinally displaced in relation to one another and that the striated rootlets (SR) are still present. AM arched membranes, N nucleus. Bar 1µm.

Fig. 3 Spermiogenesis in Clestobothrium crassiceps. **a** Longitudinal section of the spermatid during the nuclear (N) penetration showing the two axonemes longitudinally displaced in

relation to one another (Ax1 first axoneme, Ax2 second axoneme). SR striated roots. Bar 1 µm. **b,c** Longitudinal sections of a final stage of spermiogenesis showing the narrowing of the ring of arched membranes (arrows) and the appearance of the apical cone (AC) and the crested body (CB). Ax1 first axoneme, CM cortical microtubules. Bar 1 µm, Bar 0.5 µm.

Fig. 4 Diagram showing the main stages of spermiogenesis in Clestobothrium crassiceps. AC apical cone, AM arched membranes, Ax1 first axoneme, Ax2 second axoneme, C1 first centriole, C2 second centriole, CB crested body, CM cortical microtubules, DM electron-dense material, F1 first flagellum, F2 second flagellum, IB intercentriolar body, MCP median cytoplasmic process, N nucleus, SR striated rootlets.

Fig. 5 Mature spermatozoon of Clestobothrium crassiceps. **a** Longitudinal section of the anterior extremity (ASE) of the sperm cell showing the apical cone (AC) and the first axoneme (Ax1) surrounded by the crested body (CB). CM cortical microtubules. Bar 1 µm **b-f** Consecutive cross-sections of the anterior extremity of the spermatozoon from the apical cone (AC) to the beginning of the first axoneme (Ax1). Note the progressive formation of the ring of electron-dense cortical microtubules (CM). C1 first centriole, CB crested body. Bar 0.5 µm. **g** Cross-section showing the almost complete ring of electron-dense cortical microtubules around the axoneme after the disappearance of the crested body (arrowhead). Bar 0.5 µm. **h** Cross-section showing the complete ring of 30 cortical microtubules (CM) encircling the first axoneme. Bar 0.5 µm. **i-k** Consecutive cross-sections showing the gradual formation of the second axoneme (transition area between Region I and Region II). Note at the same time the progressive disorganisation of the ring of electron-dense cortical microtubules. C2 second centriole. Bar 0.5 µm. **l** Cross-section of the Region II showing the four attachment zones (arrowheads). Note the presence of only one parallel electron-lucent

cortical microtubule between the attachment points at each side of the spermatozoon. Bar 0.5 µm. **m** Cross-section of Region II showing granules of glycogen (G) and two opposite fields of parallel electron-lucent cortical microtubules (CM) between the axonemes. Bar 0.5 µm. **n** Longitudinal section of Region II showing large amounts of glycogen (G). Ax axoneme. Bar 1 µm.

Fig. 6 Mature spermatozoon of Clestobothrium crassiceps. **a** Cross-section of Region II showing the presence of glycogen (G) evidenced by the cytochemical analysis using the test of Thiéry. Bar 0.5 µm **b** Cross-section of Region III showing the nucleus (N) and two axonemes. CM cortical microtubules. Bar 0.5 µm **c** Longitudinal section of the nuclear region showing the transition area between Regions III and IV. Note the posterior extremity of the axoneme (Ax) (arrowhead). N nucleus. Bar 1 µm. **d** Cross-section of Region IV showing the disorganisation of one of the axonemes. N nucleus, S singlets. Bar 0.5 µm. **e,f** Consecutive cross-sections of the posterior area of the spermatozoon showing the reduction of the size of nucleus (N), the reduction of glycogen and the reduction in the number of cortical microtubules (CM). Bar 0.5 µm. **g,h** Consecutive cross-sections of the posterior tip of the spermatozoon showing the progressive disorganisation of the axoneme. D doublets, N nucleus, S singlets. Bar 0.5 µm. **i** Cross-section of the posterior tip of the spermatozoon showing only the nucleus (N). Bar 0.5 µm. **j** Longitudinal section of the posterior spermatozoon extremity (PSE). Note the progressive disorganization of the last axoneme (Ax) near the end of the spermatozoon body. N nucleus. Bar 1 µm.

Fig. 7 Schematic reconstruction of the mature spermatozoon of Clestobothrium crassiceps. To simplify the diagram, the granules of glycogen are not shown in the longitudinal section.

AC apical cone, ASE anterior spermatozoon extremity, Ax1 first axoneme, Ax2 second axoneme, AZ attachment zones, C1 first centriole, C2 second centriole, CB crested body, CM cortical microtubules, D doublets, G granules of glycogen, N nucleus, PM plasma membrane, PSE posterior spermatozoon extremity, S singlets.

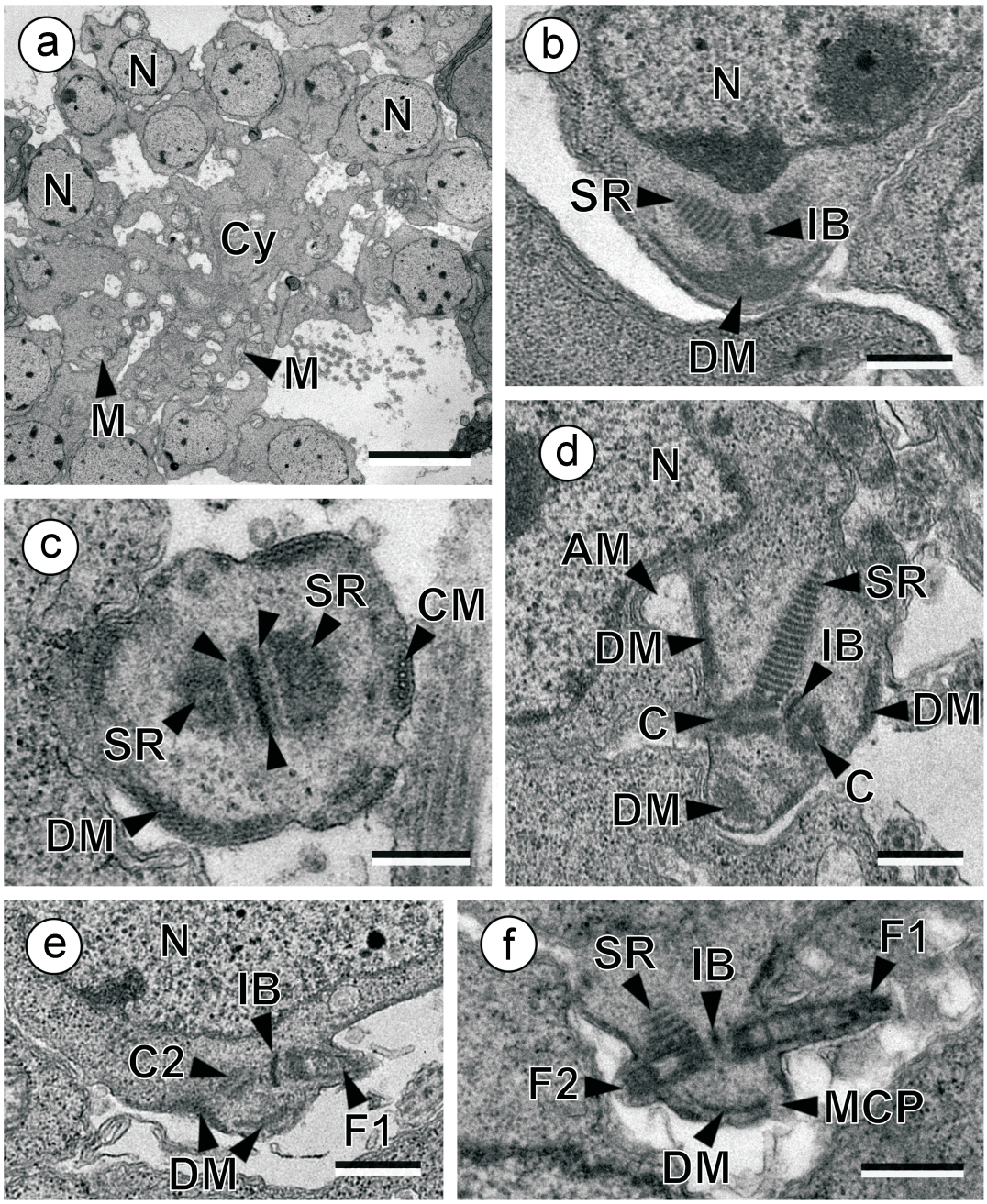
a
N
N
N
Cy
M
M
b
N
SR
IB
DM
c
SR
CM
SR
DM
d
N
AM
SR
DM
IB
C
DM
C
DM
e
N
IB
C2
F1
DM
f
SR
IB
F1
F2
MCP
DM

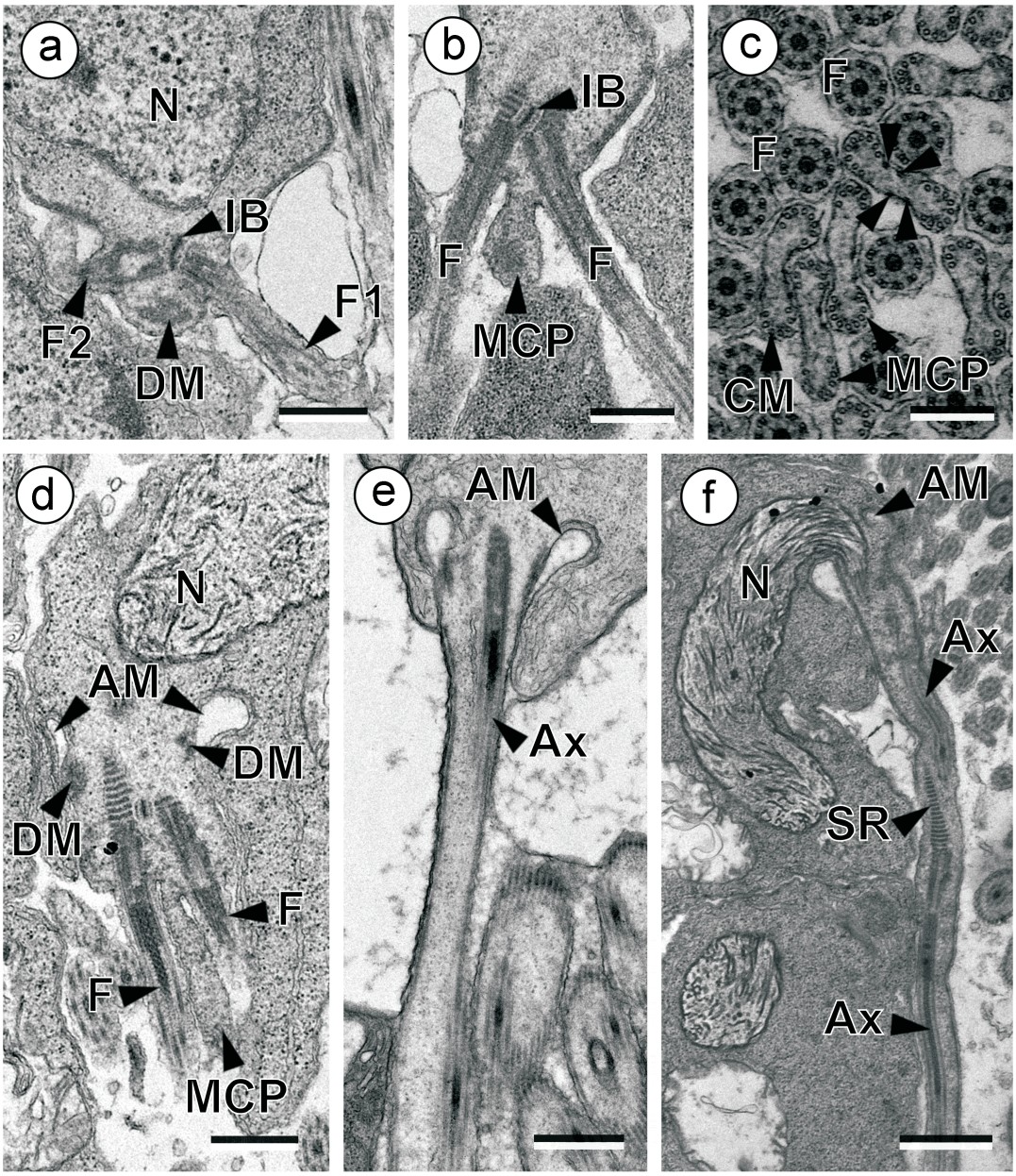
a
N
IB
F2
DM
F1
b
IB
F
F
MCP
c
F
F
CM
MCP
d
N
AM
DM
DM
F
F
MCP
e
AM
Ax
f
AM
N
Ax
SR
Ax

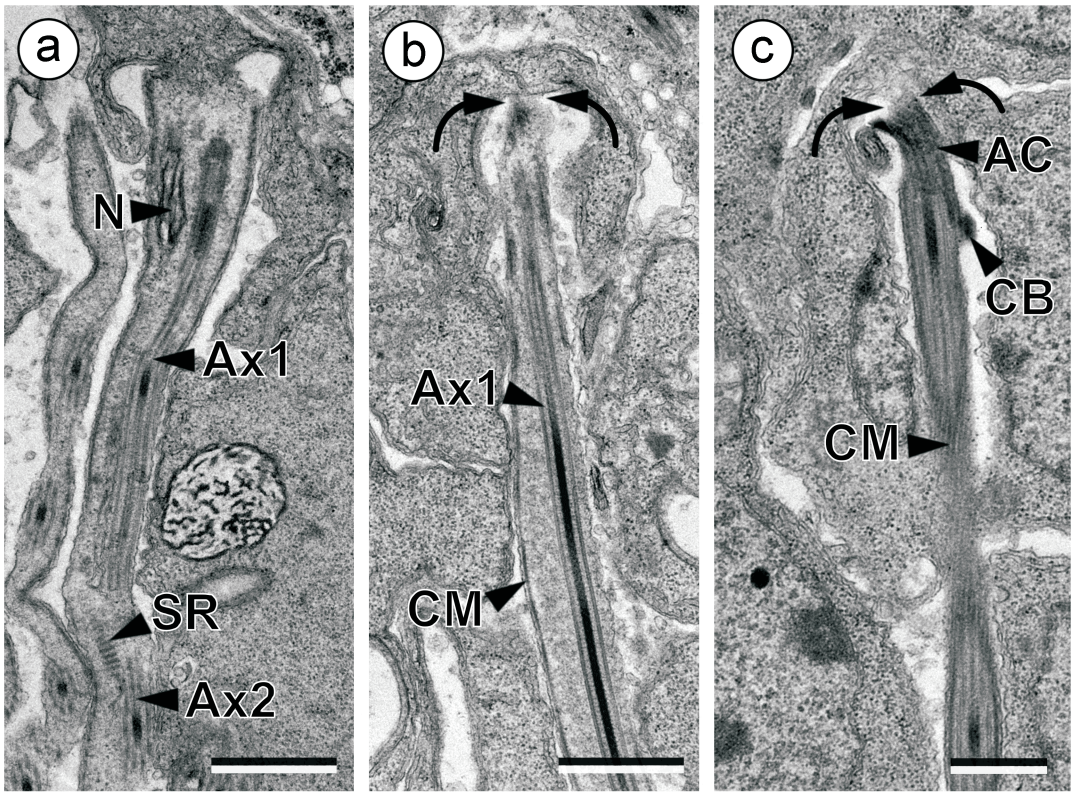
a
N
Ax1
SR
Ax2
b
Ax1
CM
c
AC
CB
CM

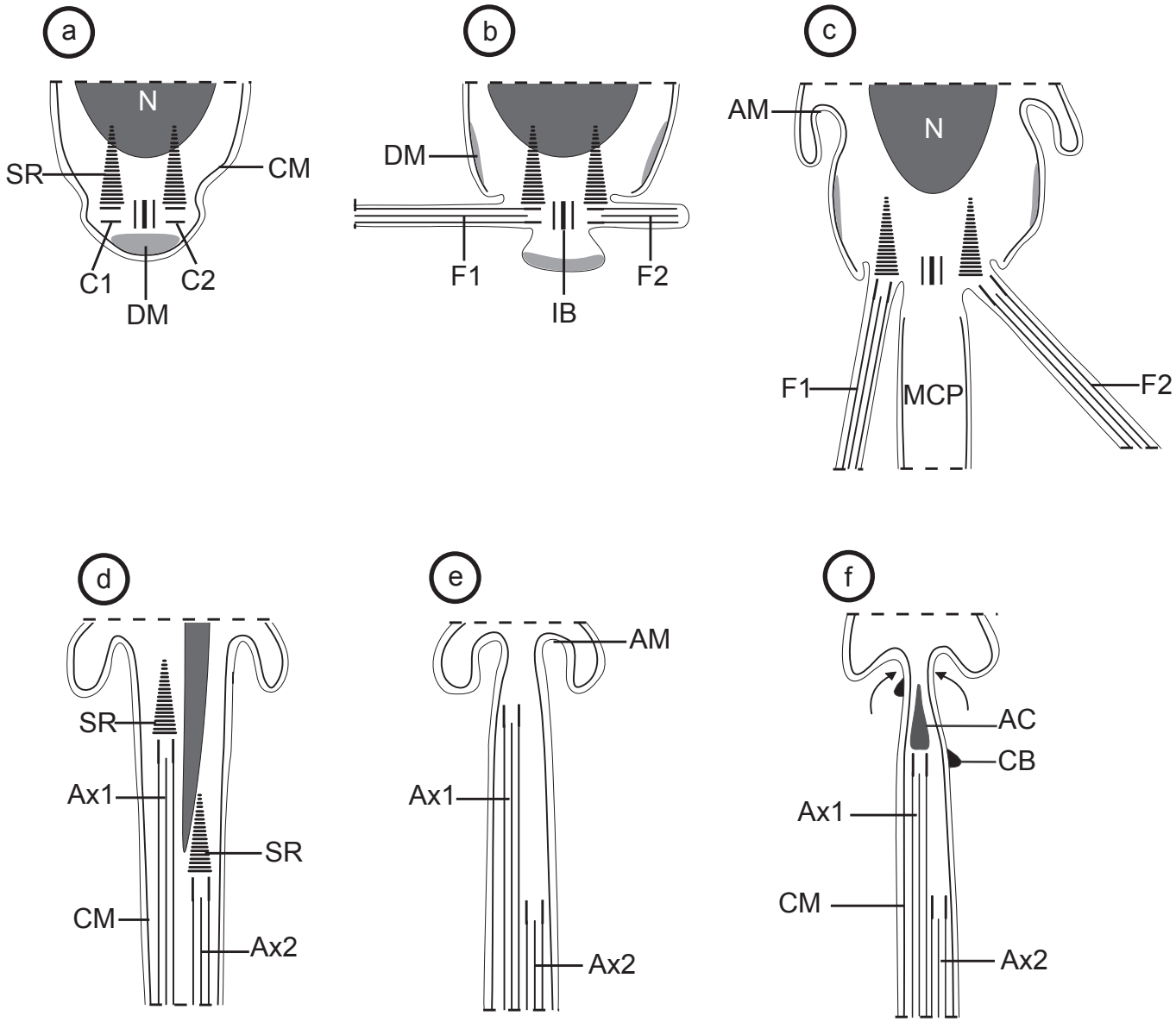
a
N
SR
CM
C1
C2
DM
b
DM
F1
F2
IB
c
AM
N
F1
MCP
F2
d
SR
Ax1
SR
CM
Ax2
e
AM
Ax1
Ax2
f
AC
CB
Ax1
CM
Ax2

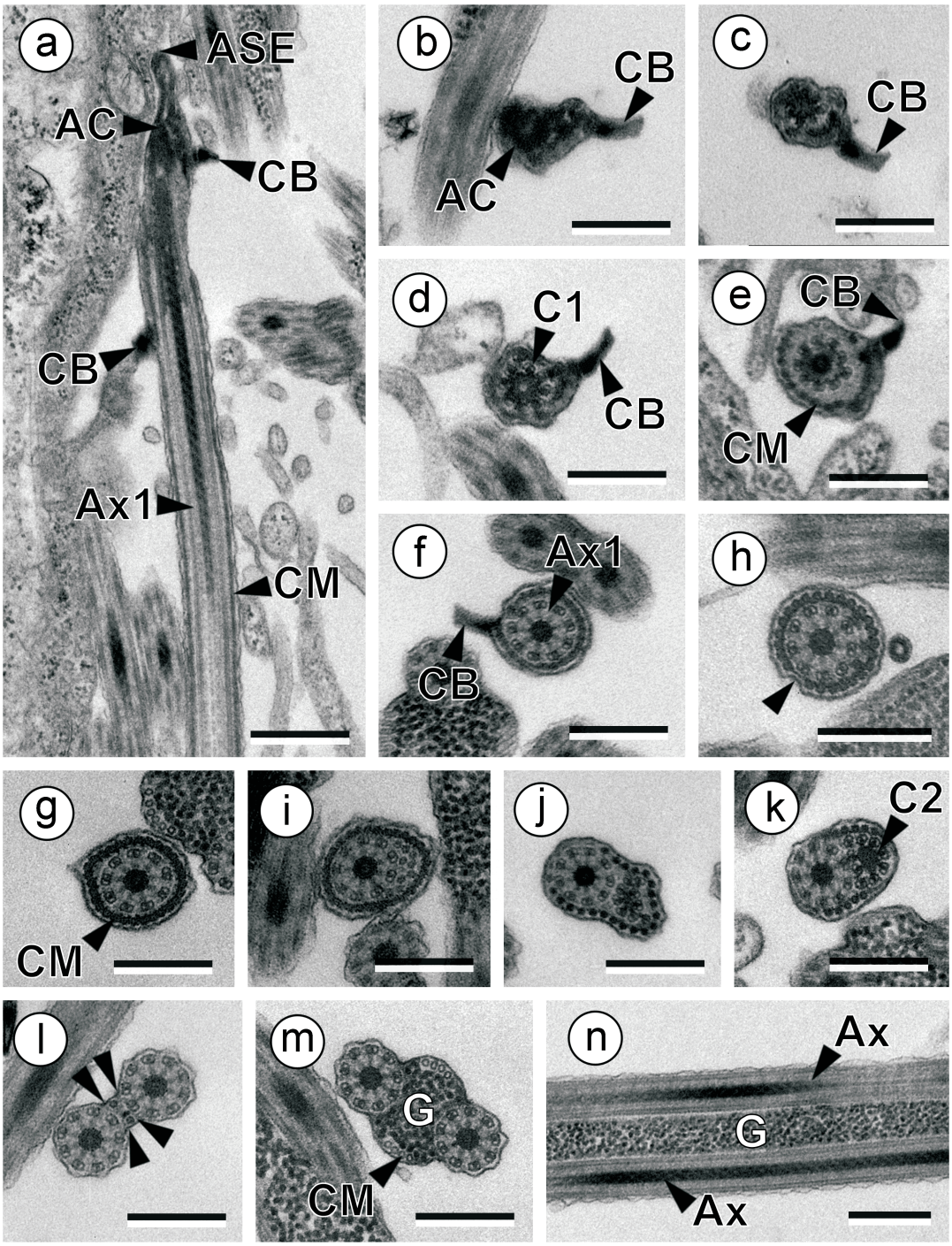
a
ASE
AC
CB
CB
Ax1
CM
b
CB
AC
c
CB
d
C1
CB
e
CB
CM
f
Ax1
CB
h
g
CM
i
j
k
C2
l
m
G
CM
n
Ax
G
Ax

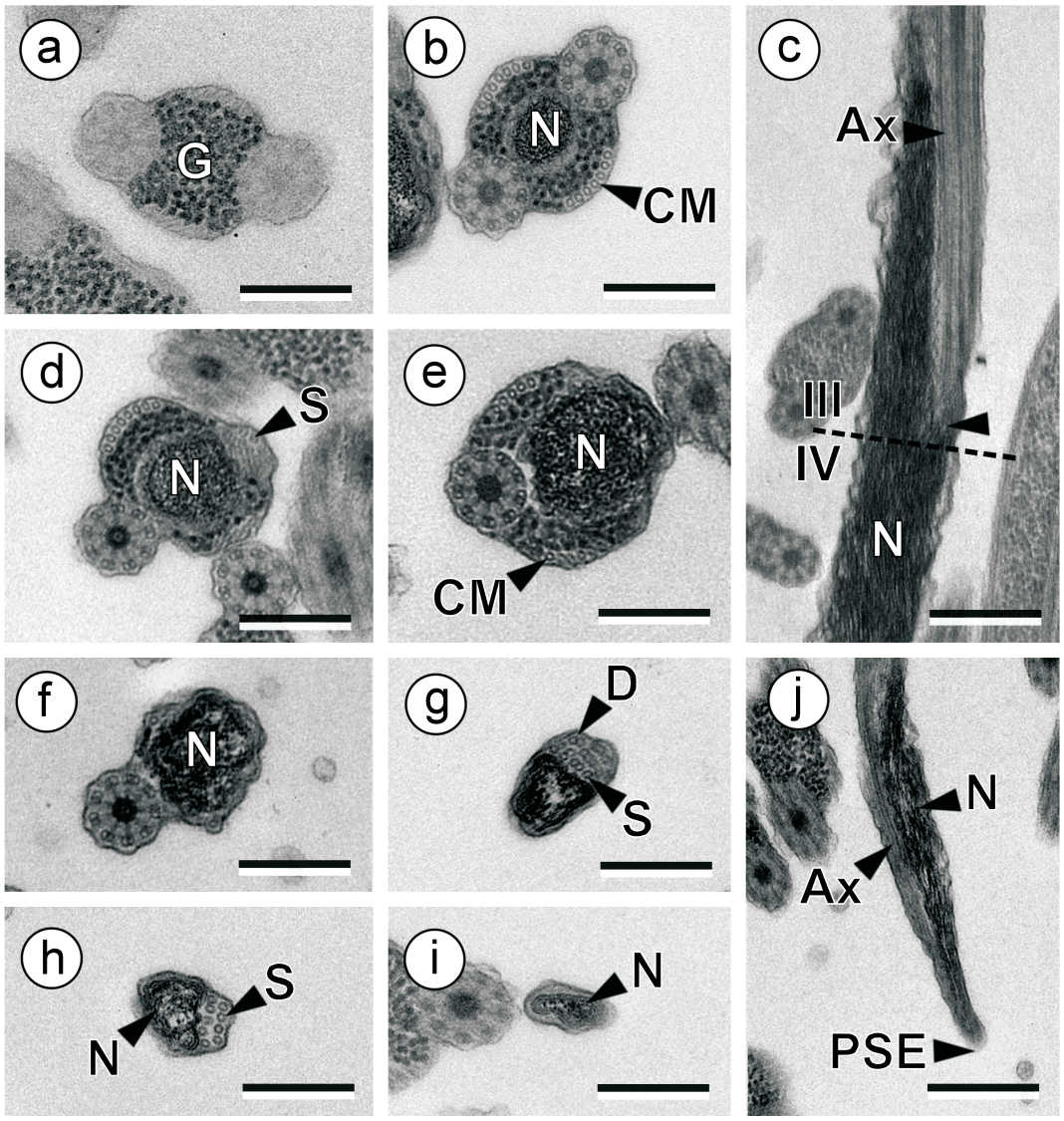
a
G
b
N
CM
c
Ax
III
IV
N
d
S
N
e
N
CM
f
N
g
D
S
j
N
Ax
PSE
h
S
N
i
N

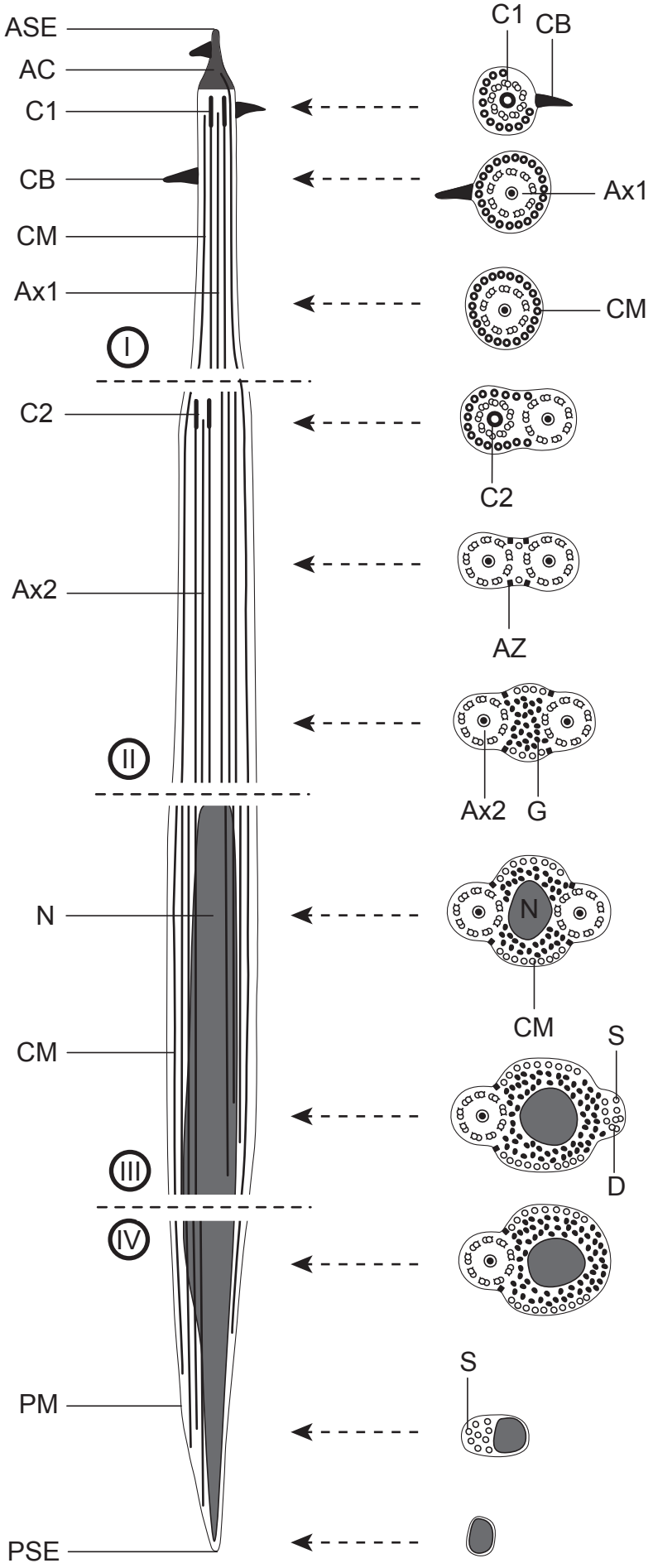
ASE
AC
C1
CB
CM
Ax1
I
C2
Ax2
II
N
CM
III
IV
PM
PSE
C1
CB
Ax1
CM
C2
AZ
Ax2
G
N
CM
S
D
S